ACCV2002: The 5th Asian Conference on Computer Vision, 23–25 January 2002, Melbourne, Australia

Simultaneous 2D images and 3D geometric model registration for texture mapping utilizing reflectance attribute

Ryo Kurazume The University of Tokyo
Ko Nishino The University of Tokyo
Zhengyou Zhang Microsoft Research, Inc.
Katsushi Ikeuchi The University of Tokyo
{kurazume,kon,ki}@cvl.iis.u-tokyo.ac.jp

Abstract

Texture mapping on scanned objects, that is, the method to map current color images on a 3D geometric model measured by a range sensor, is a key technique of photometric modeling for virtual reality. Usually range and color images are obtained from different viewing positions, through two independent range and color sensors. Thus, in order to map those color images on the geometric model, it is necessary to determine relative relations between these two viewpoints. In this paper, we propose a new calibration method for the texture mapping; the method utilizes reflectance images and iterative pose estimation based on a robust M-estimator.

Moreover, since a 2D texture image taken from one viewing point is a partial view of an object, several images must be mapped onto the object in order to cover the entire 3D geometric model. In this paper, we propose the new simultaneous registration technique of several images and geometric model based on 2D-3D edge correspondence and the epipolar constraint between images.

1 Introduction

One of the most important research issues in virtual reality (VR) is how to obtain models for virtual reality. Currently, such models are manually created by a human programmer. This manual method requires long development time and the resulting virtual reality systems are expensive. In order to overcome this problem, we have been developing techniques to automatically create virtual reality models through observation of real objects; we refer to these techniques as modeling-from-reality (MFR). The MFR method spans three aspects:

1. how to create geometric models of virtual objects
2. how to create photometric models of virtual objects
3. how to integrate such virtual objects with real or other VR scenes

For geometric modeling, we have developed a three-step method: mesh generation, alignment, and merging [7]. For photometric modeling, we have developed two rendering methods, model-based [1] and eigen-texture rendering [2], both of which automatically create such rendering models by observing real objects. For integration of virtual object with real scenes, we have developed a method that renders virtual objects based on real illumination distribution [3]. Texture mapping on scanned objects, that is, the method to map current color images on a 3D geometric model measured by a range sensor, is also a key technique of photometric modeling for virtual reality [5],[9],[10]. With the exception of several range sensors which have special configurations of optics, such as OGIS or Cyberwares, and which take both range and color images from the same viewing position, range and color images are usually obtained from different viewing positions, through two independent range and color sensors. In order to map these color images on the geometric model, it is necessary to determine the relative relationship between these two viewpoints.

In this paper, we propose a new calibration method for texture mapping using reflectance images, which are given as side products of range images for most of the range sensors. In this method, 3D reflectance edge points and 2D color edge points are first extracted from the reflectance and the color images, respectively. Then, the relative pose of each sensor is determined so that 3D reflectance edge points are aligned with the 3D points calculated from 2D color edge points by using the iterative pose estimation based on the robust M-estimator [7], [8].

Moreover, since a 2D texture image taken from one viewing point is a partial view of an object, several images must be mapped onto the object in order to cover the entire 3D geometric model. In this paper, we propose the new simultaneous registration technique of several images and geometric model based on 2D-3D edge correspondence and

geometric constraint between images, that is so called the epipolar constraint.

2 Related work

For alignment of range and color images, Viola proposed a technique based on a statistical method [6]. Allen et al. also proposed a method using the intersection lines of several planes extracted from the range data and the color edges [5]. Several object recognition algorithms also can be used to align range edges with intensity edges[7],[8]. These methods work well on the surface with little albedo variance. But these are highly likely to be trapped to a local minimum on surfaces with rich textures.

Elstrom et al. proposed an alignment method using reflectance images [4]. This method can be summarized as follows:

1. Extract feature points from the reflectance and intensity images by the use of a corner detector.
2. Determine correspondence between these feature points by calculating the similarity based on gray level subtraction and shape of corners.
3. Estimate the relative pose roughly by solving the closed form equation derived from the determined correspondence.
4. Estimate the relative pose precisely by comparing the depth of feature points obtained by a stereo calculation using reflectance and intensity images, with the feature point depth obtained by a laser measurement.

This method works well in cases where the object consists of flat planes with few texture patterns and only simple line edges are extracted. However, the corner detector has low reliability for the object that consists of curved surfaces. In addition, it is difficult to determine good correspondence of feature points between the reflectance and intensity images, which are obtained from different configurations of optics. Furthermore, since contour lines of curved surfaces depend on a viewing direction, the contour edges of the reflectance image do not directly correspond with the contour edges of the color image. Thus, for accurate pose estimation, these contour edges should be removed in advance from the extracted reflectance edges.

3 Aligning a texture on range data

One simple solution for determining the relationship between range and color images is through calibration using the calibration board and fixtures. However, this method requires that the range and color sensors be fixed on the fixture once the relationship is calibrated. Such a fixed structure is inconvenient. Usually, a color camera is much handier than a range sensor. We prefer to take color images freely without having to transport a heavy range sensor.

Generally speaking, range sensors often provide reflectance images as side products of range images. A reflectance image is given as a collection of the strength of returned laser energy at each pixel. This reflectance image is aligned with the range image because both images are obtained through the same receiving optical device. The returned timing provides a depth measurement, while the returned strength provides a reflectance measurement. Thus, this reflectance image is commonly available in a wide variety of range sensors, including ERIM, Perceptron, and our main sensor, Cyrax.

We decided to employ this reflectance image as a vehicle for the alignment of range images with intensity images. Reflectance images are similar to intensity images in that both images are somehow related by surface roughness. As mentioned above, the reflectance image is aligned with the range image. Thus, to align the reflectance image with the intensity image is a much easier task than that of aligning the range image with the intensity image.

More precisely, we align edges extracted from reflectance images by the Canny operator with those in intensity images so that 3D position error of those edges is minimized by the iterative calculation. Edges in reflectance images are generated due to several reasons. A boundary between two different colors or materials generates a discontinuity of reflectance and, thus, an edge in a reflectance image. For instance, since our Cyrax range scanner uses a green laser diode, reflectance edges can be observed along the boundary between two colors or materials which have the different reflectance ratios for this wavelength. Since different materials are of different colors, a discontinuity also appears in the color images. In particular, an intensity image with the same wavelength as that of a laser scanner, the G channel for our Cyrax range scanner, has robust similarities with the reflectance images. Jump edges along small ranges in a range image also appear as jump edges in reflectance images. Such jump edges often provide small shadow regions alongside themselves and are also observed as edges in intensity edges. Occluding boundaries are observed in reflectance and intensity images. By aligning the discontinuities in reflectance images with those in intensity images, we can determine the relative relationship between the range and intensity views.

Prior to doing the alignments, we paste the necessary reflectance edges onto the 3D geometric model. As mentioned above, since the occluding boundaries vary depending on the viewing direction, the edges along the occluding boundaries are previously removed from the reflectance images. However, the edges along the current occluding

boundaries can be estimated from the 3D geometric model and the current viewing direction. Our algorithm extracts them automatically, and uses them for the alignment. Thus, this alignment problem is the one between:

- 3D reflectance edges existing on 3D range surfaces
- 3D edges along the occluding boundaries existing on 3D range surfaces

and

- 2D edges in the 2D intensity image

Extracted edges are represented as a collection of points along them as shown in Fig.1. Consequently, the alignment is done between 3D points on 3D range surfaces and 2D points in the 2D image, that is, as the alignment between 3D and 2D points.

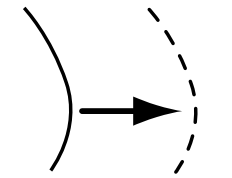

Figure 1: Edge sampling

The three steps in the 3D-2D alignment are as follows:

1. Extract possible observable reflectance edges on 3D reflectance images and edges along the occluding boundaries based on the current viewing direction.
2. Establish correspondences between 3D edges and 2D intensity edges.
3. Determine the relative relationship iteratively based on the correspondences.

3.1 Visibility calculation and correspondences

Applying Canny operators to the reflectance images enables us to obtain reflectance edges. These are then sampled to edge sampling points, and stored on the surface of the 3D geometric model. First, the system decides which edge part is visible from the current viewing direction. Visibility of an edge point, P_i, can be examined as

$$P_i = \begin{cases} visible \cdots n \cdot v \geq 0 \\ invisible \cdots otherwise \end{cases} \quad (1)$$

where n is the surface normal of the patch and v is the current camera's viewing direction with respect to the current 3D geometric model. The edges along the occluding boundary will also be sampled into edge points along the occluding boundary, which is detected as

$$P_i = \begin{cases} edge \cdots 0 < n \cdot v \leq t \\ not\ edge\ \cdots otherwise \end{cases} \quad (2)$$

where t is a threshold. Pruning of small edges is necessary. Currently, by adjusting various parameters in edge tracking, we remove small edges and extract only dominant edges.

3.2 Correspondences

To establish correspondence, the system projects 3D edge points onto the 2D image plane. Then, the system finds the nearest 2D edge points on the image plane. This point pair will be used to evaluate the value of the error function in next step.

3.3 Pose estimation by M-estimator

To determine the relative pose that coincides the position of 2D intensity edges and 3D edges, we use the M-estimator, which is one of the robust estimators.

First, the distance between corresponding 2D intensity edge points and 3D edge points is evaluated as shown in Fig.2: where z_i is a 3D error vector which is on a perpendicular line from a 3D edge point to the stretched line between the optical center and a 2D edge point on the image plane.

$$\epsilon_i = Z_i \sin\theta \quad (3)$$

where Z_i is the distance between the optical center and 3D edge point, and θ is the angle between 2D intensity edge point and 3D edge point.

The system finds the configuration, P, which minimizes the total error, E,

$$E(P) = \sum_i \rho(\epsilon_i) \quad (4)$$

where ρ is an error function. The minimum of $E(P)$ can be obtained by:

$$\frac{\partial E}{\partial P} = \sum_i \frac{\partial \rho(\epsilon_i)}{\partial \epsilon_i} \frac{\partial \epsilon_i}{\partial P} = 0 \quad (5)$$

We can consider $w(\epsilon)$ as a weight function to evaluate error terms.

$$w(\epsilon) = \frac{1}{\epsilon} \frac{\partial \rho}{\partial \epsilon} \quad (6)$$

Thus, the minimization can be derived as the following least squared equation:

$$\frac{\partial E}{\partial P} = \sum_i w(\epsilon_i)\epsilon_i \frac{\partial \epsilon_i}{\partial P} = 0 \quad (7)$$

We choose the Lorentzian function for this function.

$$w(\epsilon) = \left(1 + \frac{1}{2}\left(\frac{\epsilon}{\sigma}\right)^2\right)^{-1} \quad (8)$$

By solving this equation using the conjugate gradient method, we can obtain the configuration P that minimizes the error term and gives the relative relationship between the camera and range sensor.

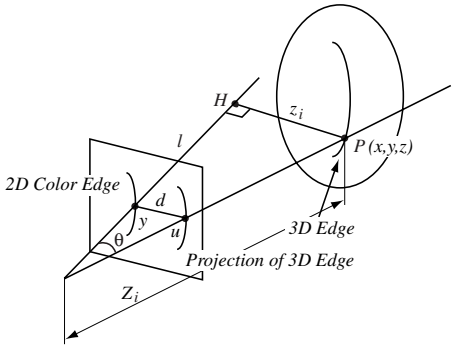

Figure 2: 2D distance and 3D distance

3.4 Experiment

3.4.1 Computer simulation

In order to verify the performance of the proposed 2D-3D alignment method, the computer simulation was carried out. In this simulation, we assumed that a cylinder with 100 mm diameter and 200 mm length was placed 1000 mm ahead of the color and range sensors. We did not assume the reflectance values obtained from the range sensor, and used 3D edge points along the occluding boundaries only. The resolution of the color sensor was 300 dpi and focus length was 70 mm.

Fig.3 shows the simulation model, and Fig.4 shows the process of the alignment.

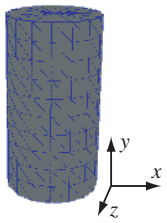

Figure 3: Simulation model

From several initial poses with maximum 50 mm and 20 degrees difference from the actual pose, the optimum pose was calculated. Table 1 shows the obtained average and the standard deviation of the estimated position and the inclination of the y axis after 10 simulations.

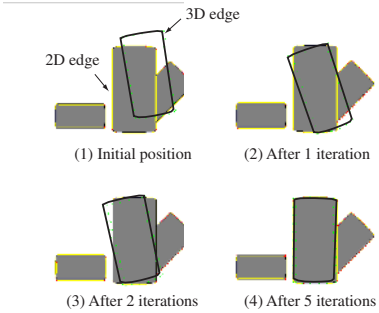

Figure 4: Simulation results

Table 1: Position errors [mm (pixel)]

	x	y	z	θ[deg.]
Average	0.14 (0.12)	-0.20 (0.16)	-967.81	4.0
STD.	0.13 (0.11)	1.89 (1.56)	5.94	4.1

In Table 1, the depth of the z axis is calculated closer than the actual position. This is because 3D edge points along the occluding boundaries are obtained as the center of triangle patches which satisfy Eq.2, and these center points are calculated inside the actual boundaries. Thus, if the triangle patches were to be set more densely, this would not be a problem.

As a result of this simulation, it wass verified that the accurate relative pose between the camera and the range sensor can be estimated by the proposed 3D-2D alignment method.

3.4.2 Texture mapping of a dish with drawing

Next, using the Cyrax laser scanner , we attempted the texture mapping of a dish with drawing.

Fig.5 shows the reflectance image and extracted reflectance edges, and Fig.6 shows the color texture image taken by the digital camera (Nikon, D1) along with the extracted intensity edges. Here, as shown in Fig.5, the brighter the pixel color is, the larger its reflectance.

Fig.7 shows the procedure of the alignment of the reflectance and intensity images through the use of the M-estimation method. For these symmetrical objects, accurate alignment which coincides with the position of the drawing is impossible for the conventional methods which use the geometric edges extracted from the geometric model or the CAD model. On the other hand, our proposed method can perform accurate alignment due to the use of reflectance information obtained from the drawing as shown in Fig.8

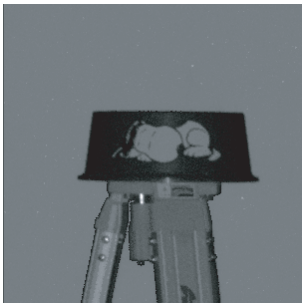

(a) Reflectance image

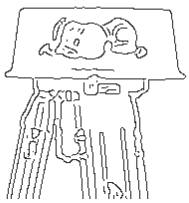

(b) Reflectance edges

Figure 5: Reflectance image of the dish

(a) Color image

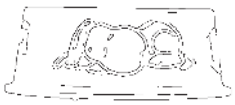

(b) Intensity edges

Figure 6: Texture image of the dish

3.4.3 Texture mapping of Great Buddha of Kamakura

We have recently developed a method for preserving Japanese cultural heritage objects. Using accurate laser scanners [11], 3D digital models of these objects are created through observation. For our first preservation project, we have created a 3D geometric model of the Great Buddha of Kamakura as shown in Fig.9.

Using our proposed alignment method, we tried to map the color texture image taken from the digital camera onto this model. Fig.10 shows the reflectance image and extracted reflectance edges, Fig.11 shows the color texture image taken by the digital camera. Fig.12 shows the procedure for the alignment of the reflectance and intensity images through the use of the M-estimation method.

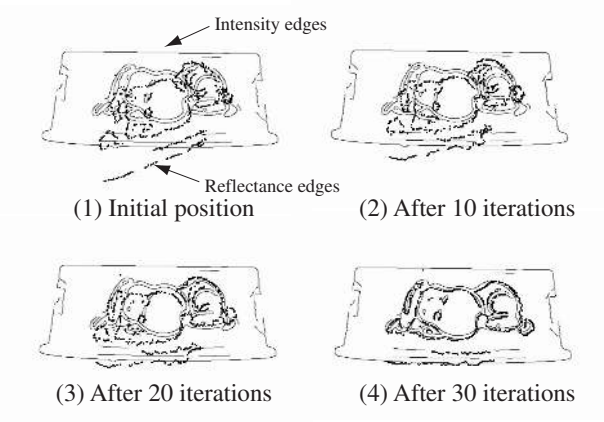

Figure 7: Intensity edges aligned with reflectance edges

Figure 8: Aligned color texture on the dish

Figure 9: Geometric model of the Great Buddha of Kamakura

By comparing Fig.10 and Fig.11, the reflectance and the color image have robust similarities, for example, the shapes of rust on the forehead or the junctures of bronze. Fig.13 shows the result of the mapping of the current color texture onto the 3D geometric model.

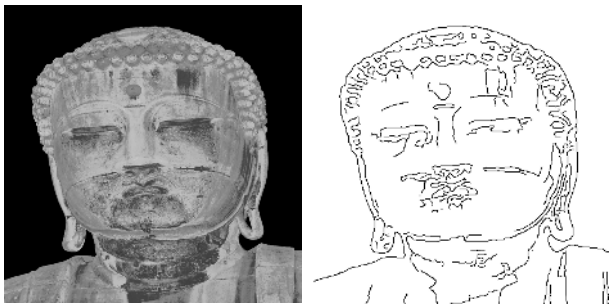

Figure 10: Reflectance image of the Great Buddha of Kamakura

4 Simultaneous registration using geometric constraint

The 2D-3D registration technique proposed above is for the alignment between one texture image and a geometric model. However, since a 2D texture image taken from one viewing point is a partial view of an object, several images must be mapped onto the object in order to cover the en-

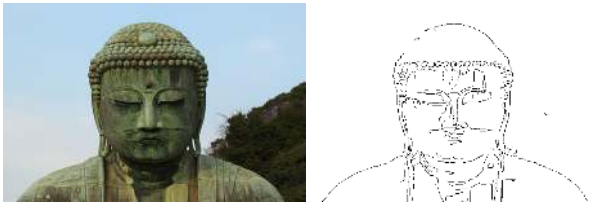

Figure 11: Texture image of the Great Buddha of Kamakura

Figure 12: Aligned intensity edges with reflectance edges

tire 3D geometric model. One simple method to align the several images and the geometric model is to utilise the proposed 2D-3D registration technique for each image sequentially. However, as the additional criterion, we can utilize the geometric constraint between these texture images, that is so called the epipolar constraint [12].

Let's consider the case that the two texture images, 1 and 2, which are taken from the two different viewing points, are going to be mapped. First, we define the world coordinate system $\mathbf{\Sigma}_w$ and two camera coordinate systems that is fixed on each viewing point, $\mathbf{\Sigma}_1$ and $\mathbf{\Sigma}_2$, as shown in Fig.14. Point $\tilde{\mathbf{M}}_w = (x_w, y_w, z_w, 1)^T$, which is an arbitrary point expressed in the world coordinate system, is projected on each image plane as points $\tilde{\mathbf{m}}_1 = (x_1, y_1, 1)^T$ and $\tilde{\mathbf{m}}_2 = (x_2, y_2, 1)^T$ according to the following equations.

$$s\tilde{\mathbf{m}}_1 = \mathbf{P}_1\tilde{\mathbf{M}}_w \tag{9}$$

$$s\tilde{\mathbf{m}}_2 = \mathbf{P}_2\tilde{\mathbf{M}}_w \tag{10}$$

Where, $\mathbf{P}_1$ and $\mathbf{P}_2 \in R^{3\times 4}$ are the projection matrixes consisting of the internal and external camera parameters.

Figure 13: Aligned color texture on the 3D geometric model

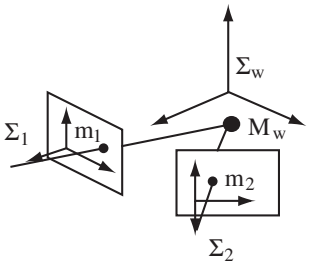

Figure 14: Coordinate systems

Using the pseudo inverse $\mathbf{P}_2^\dagger$ of the projection matrix $\mathbf{P}_2$, Eq.(10) is changed as

$$\begin{aligned}\tilde{\mathbf{M}}_w &= s\mathbf{P}_2^\dagger\tilde{\mathbf{m}}_2 + (\mathbf{I} - \mathbf{P}_2^\dagger\mathbf{P}_2)\xi \\ &= s\mathbf{P}_2^\dagger\tilde{\mathbf{m}}_2 + \mathbf{p}_{2,null}\end{aligned} \tag{11}$$

Where, $\mathbf{p}_{2,null}$ is the position of the focus of the camera 2 expressed in the world coordinate system. By substituting Eq.(11) into Eq.(9), we can derive

$$\begin{aligned}s\tilde{\mathbf{m}}_1 &= s\mathbf{P}_1(\mathbf{P}_2^\dagger\tilde{\mathbf{m}}_2 + \mathbf{p}_{2,null}) \\ &= s\mathbf{P}_1\mathbf{P}_2^\dagger\tilde{\mathbf{m}}_2 + \mathbf{P}_1\mathbf{p}_{2,null} \\ &= s\mathbf{P}_1\mathbf{P}_2^\dagger\tilde{\mathbf{m}}_2 + \mathbf{e}_1\end{aligned} \tag{12}$$

Where, $\mathbf{e}_1$ is called as the "epipole", which is the crossing point of the line connecting the focus points of both cameras, and the image plane of camera 1. Beside, by multiplying $[\mathbf{e}_1\times]$ and $\mathbf{m}_1^T$ for both sides of the equation, the following equation can be derived.

$$\begin{aligned}s[\mathbf{e}_1\times]\tilde{\mathbf{m}}_1 &= s[\mathbf{e}_1\times]\mathbf{P}_1\mathbf{P}_2^\dagger\tilde{\mathbf{m}}_2 + [\mathbf{e}_1\times]\mathbf{e}_1 \\ &= s[\mathbf{e}_1\times]\mathbf{P}_1\mathbf{P}_2^\dagger\tilde{\mathbf{m}}_2\end{aligned} \tag{13}$$

$$\tilde{\mathbf{m}}_1^T[\mathbf{e}_1\times]\tilde{\mathbf{m}}_1 = \tilde{\mathbf{m}}_1^T[\mathbf{e}_1\times]\mathbf{P}_1\mathbf{P}_2^\dagger\tilde{\mathbf{m}}_2 \tag{14}$$

The left side of this equation is always 0. Consequently, we can obtain the next equation.

$$\tilde{\mathbf{m}}_1^T[\mathbf{e}_1\times]\mathbf{P}_1\mathbf{P}_2^\dagger\tilde{\mathbf{m}}_2 = 0 \tag{15}$$

$$\tilde{\mathbf{m}}_1^T\mathbf{F}\tilde{\mathbf{m}}_2 = 0 \tag{16}$$

Where, $\mathbf{F}$ is called as the fundamental matrix [12].

$$\mathbf{F} = [\mathbf{e}_1 \times]\mathbf{P}_1\mathbf{P}_2^{\dagger} \tag{17}$$

On the image plane of the camera 1, radial lines from the epipole can be written as

$$\tilde{\mathbf{m}}_2^T \mathbf{F} \tilde{\mathbf{m}}_1 = \mathbf{l}_1 \tilde{\mathbf{m}}_1 = 0 \tag{18}$$

These lines are called as epipolar lines. Therefore, if the corresponding points on both images, $\tilde{\mathbf{m}}_1$ and $\tilde{\mathbf{m}}_2$, are determined, the distance between the point $\tilde{\mathbf{m}}_1$ and the epipolar line corresponding to the point $\tilde{\mathbf{m}}_2$ on image plane 1 can be calculated as

$$d_1 = \frac{\mid \mathbf{l}_1 \tilde{\mathbf{m}}_1 \mid}{\sqrt{l_{1,x}^2 + l_{1,y}^2}} = \frac{\mid \tilde{\mathbf{m}}_2^T \mathbf{F} \tilde{\mathbf{m}}_1 \mid}{\sqrt{l_{1,x}^2 + l_{1,y}^2}} \tag{19}$$

In the same manner, the distance of the epipolar line and the corresponding point on the image plane 2 is given as

$$d_2 = \frac{\mid \tilde{\mathbf{m}}_1^T \mathbf{F}^T \tilde{\mathbf{m}}_2 \mid}{\sqrt{l_{2,x}^2 + l_{2,y}^2}} \tag{20}$$

Therefore, the total distance of these corresponding points is obtained as

$$\begin{aligned} \epsilon &= \frac{(\tilde{\mathbf{m}}_2^T \mathbf{F} \tilde{\mathbf{m}}_1)^2}{l_{1,x}^2 + l_{1,y}^2} + \frac{(\tilde{\mathbf{m}}_1^T \mathbf{F}^T \tilde{\mathbf{m}}_2)^2}{l_{2,x}^2 + l_{2,y}^2} \\ &= w^2 (\tilde{\mathbf{m}}_2^T \mathbf{F} \tilde{\mathbf{m}}_1)^2 \end{aligned} \tag{21}$$

where,

$$w = \left(\frac{1}{l_{1,x}^2 + l_{1,y}^2} + \frac{1}{l_{2,x}^2 + l_{2,y}^2} \right)^{\frac{1}{2}} \tag{22}$$

Equation (21) shows the geometric constraint of the focus position of the images 1 and 2, and is called as the "epipolar constraint".

Therefore, simultaneous registration of two 2D texture images and the 3D geometric model is formulated as the minimization problem of total error defined by next equation.

$$\begin{aligned} \min_{\mathbf{P}_1, \mathbf{P}_2} E &= \sum_i \rho(\epsilon_{1,i}^{2D-3D}(\mathbf{P}_1)) + \sum_j \rho(\epsilon_{2,j}^{2D-3D}(\mathbf{P}_2)) \\ &\quad + \sum_k \rho(\epsilon_k^{2D-2D}(\mathbf{P}_1, \mathbf{P}_2)) \end{aligned} \tag{23}$$

where, $\rho(\epsilon_{1,i}^{2D-3D}(\mathbf{P}_1))$ and $\rho(\epsilon_{2,j}^{2D-3D}(\mathbf{P}_2))$ are the errors of the 2D-3D registration defined in Eq.(4), $\rho(\epsilon_k^{2D-2D}(\mathbf{P}_1, \mathbf{P}_2))$ is the error derived from the epipolar constraint of both images as Eq.(21), and ρ is the error function.

To calculate the optimum poses $\mathbf{P}_1$ and $\mathbf{P}_2$ that minimize the error defined by Eq.(23), corresponding points of both images must be determined beforehand. We can consider two kinds of corresponding point detection methods as follows:

- Corresponding regions based on the similarity calculation of both images.
- Selected edge points on each image for the calculation of 2D-3D alignment proposed in Section 3.

In the following experiments, we adopted the method based on the similarity calculation.

Figure 15 shows the two texture images of the dish and Figures 16 and 17 show the procedure of the simultaneous and the separate registration of two texture images and a geometric model of a dish, respectively. The epipolar lines for only three corresponding points are also shown in Figures 16. 12 corresponding points, depicted as the small rectangles in Figure 15, were calculated using KLT method [13]. In Figure 17, the registration processes were executed separately for each image without the use of epipolar constraint, and it is clear that the registration of iamge 2 was failed due to the local minimum. Figure 18 shows the mapping results for each texture image and both images onto the geometric model of the dish.

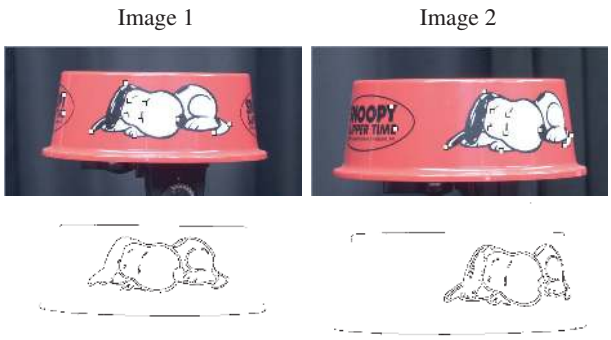

Figure 15: Two color images of the dish

5 Conclusions

In this paper, we proposed a new calibration method for texture mapping through the use of reflectance images, which are given as side products of range images for most range sensors. In this method, 3D reflectance edge points and 2D color edge points are first extracted from the reflectance image and the color image, respectively. Then, the relative pose of each sensor is determined so that the 3D reflectance edge points coincide with the 3D points calculated from the 2D color edge points be the use of the robust M-estimator. Furthermore, we propose the new simultaneous registration technique of several texture images and geometric model

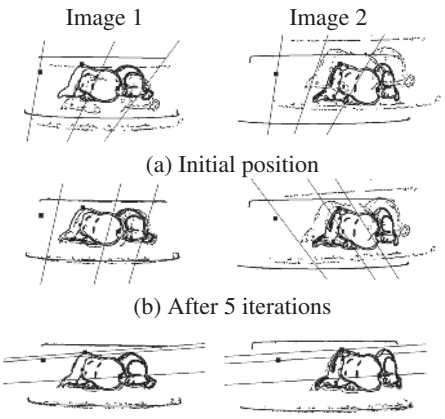

Figure 16: Simultaneous registration using epipolar constraint

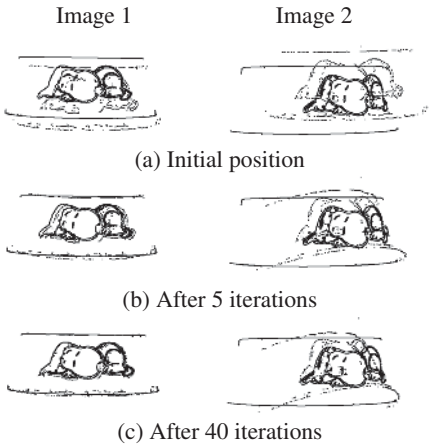

Figure 17: Separate registration without epipolar constraint

based on 2D-3D edge correspondence and the epipolar constraint between images.

Using the proposed method, experiments of the texture mapping for a symmetrical dish and the 3D geometric model of Great Buddha of Kamakura were carried out, and the usefulness of the proposed method was verified.

Acknowledgments

This project is funded by Core Research for Evolutional Science and Technology (CREST) of Japan Science and Technology Corporation (JST).

References

[1] Y. Sato, M. D. Wheeler, and K. Ikeuchi, "Object shape and reflectance modeling from observation", Proceedings of ACM SIGGRAPH 97, In Computer Graphics Proceedings, Annual Conference Series 1997, ACM SIGGRAPH, pp.379-387, August 1997.

[2] K.Nishino, Y.Sato and K.Ikeuchi, "Eigen-Texture Method: Appearance Compression based on 3D Model", in Proc. of Computer Vision and Pattern Recognition '99, vol.1, pp.618-624, Jun., 1999.

[3] I. Sato, Y. Sato, and K. Ikeuchi, "Acquiring a radiance distribution to superimpose virtual objects onto a real scene," IEEE Trans Visualization and Computer Graphics, Vol. 5, No. 1, pp.1-12, January 1999.

[4] Mark D. Elstrom and Philip W. Smith,Stereo-Based Registration of Multi-Sensor Imagery for Enhanced Visualization of Remote Environments,Proceedings of the 1999 IEEE International Conference on Robotics & Automation, pp.1948-1953, 1999.

[5] Ioannis Stamos and Peter K. Allen, Integration of Range and Image Sensing for Photorealistic 3D Modeling, Proceedings of the 2000 IEEE International Conference on Robotics and Automation, pp.1435-1440, 2000.

[6] P. Viola and W.M. Wells III, Alignment by maximization of mutual information, International Journal of Computer Vision, Vol.24, No.2, pp.137-154, 1997.

[7] M. D. Wheeler, "Automatic Modeling and Localization for Object Recognition", Technical Report (Ph.D. Thesis), CMU-CS-96-188, School of Computer Science, Carnegie Mellon University, October, 1996.

[8] M. D. Wheeler and Katsushi Ikeuchi, "Sensor Modeling, Probabilistic Hypothesis Generation, and Robust Localization for Object Recognition", IEEE Transactions on Pattern Analysis and Machine Intelligence ,Vol. 17, No. 3, March 1995.

[9] P. Debevec, D.J. Taylor, and J. Malik, Modeling and rendering architecture from photographs; A hybrid geometry and image-base approach, Proc. of SIGGRAPH'96, pp.11-20, 1996.

[10] P. Debevec, Y. Yu, and G. Borshukov, Efficient view-dependent image-based rendering with projective texture-mapping 9th Eurographics workshop on rendering, pp.105-116, 1998.

[11] Daisuke Miyazaki, Takeshi Ooishi, Taku Nishikawa, Ryusuke Sagawa, Ko Nishino, Takashi Tomomatsu, Yutaka Takase, Katsushi Ikeuchi,The Great Buddha Project: Modelling Cultural Heritage through Observation,VSMM2000 (6th international conference on virtual systems and multimedia), pp.138-145, 2000.

[12] Z.Zhang, R. Deriche, O. Faugeras and Q,T, Kuong, A robust technique for matching two uncalibrated images through the recovery of the unknown epipolar geometry. *Artificial Intelligence Journal*, 78: 87-119, 1995.

[13] Jianbo Shi and Carlo Tomasi, Good Features to Track, IEEE Conference on Computer Vision and Pattern Recognition, pp.593-600, 1994.

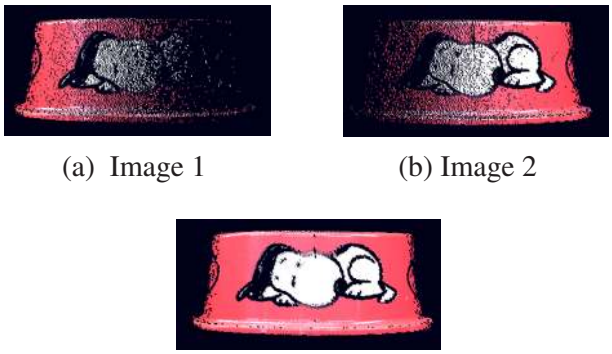

Figure 18: Mapped texture images